International Journal of Applied and Advanced Scientific Research (IJAASR)
Impact Factor: 5.655, ISSN (Online): 2456 - 3080
(www.dvpublication.com) Volume 2, Issue 2, 2017

STUDIES ON PERFORMANCE OF BACK FED 2-6 GHZ LINEAR ARRAYS OF H-PLANE SECTORAL HORNS

Chandana Viswanadham* & Prudhvi Mallikarjuna Rao**
* Ph.D Student, Andhra University, Visakhapatnam, Andhra Pradesh
** Professor, Department of ECE, Andhra University, Visakhapatnam, Andhra Pradesh

Cite This Article: Chandana Viswanadham & Prudhvi Mallikarjuna Rao, "Studies on Performance of Back Fed 2-6 GHZ Linear Arrays of H-Plane Sectoral Horns", International Journal of Applied and Advanced Scientific Research, Volume 2, Issue 2, Page Number 229-239, 2017

Abstract:

The popular electronic systems like Satellite transponders, Radars, jammers, trackers, communication systems, etc., were designed with phased array antennas in their transmitter and or receiver sections, to provide electronically steered beams through passive and active beam steering techniques. In this paper, the performance of eight elements linear array of sectoral horns, is studied, simulated and results are presented. The design of the array with eight sectoral horn elements is carried out with changes in the parameters and configurations to obtain the improvements in the specifications. The comparison of the simulation results are presented in this paper.

Indexed Terms: Band Width Ratio (BWR), Impedance, Jammer, Matching Networks, Rotman Lens & Ultra Wide Band (UWB)

1. Introduction:

The present Electronic Counter Measures (E.C.M) systems are configured with high power transmitters consisting of Digital Radio Frequency Memory (D.R.F.M), high power microwave amplifiers and highly directive and electronically steerable antenna [1-2]. The active V.S.W.R of the array is very critical parameter in these applications and depends on V.S.W.R of each element in the array. The scientists and engineers have suggested different techniques to improve V.S.W.R of pyramidal horns, such as dielectric loading, stub matching, etc., [3 – 5]. But these techniques reduce the gain to some extent and hence results in low E.R.P. In this paper, the design and simulation of various configurations of Rotman lens fed 2-6 GHz linear array of H-plane sectoral horns is presented with improved performance for V.S.W.R, gain, side lobe levels, etc.,. Comparison of these different techniques is presented in the paper.

2. Design Equations:

2.1 Design Equation: The geometry of H-plane sectoral horn antenna is shown at "Fig. 1" [3 - 4] along with design parameters.

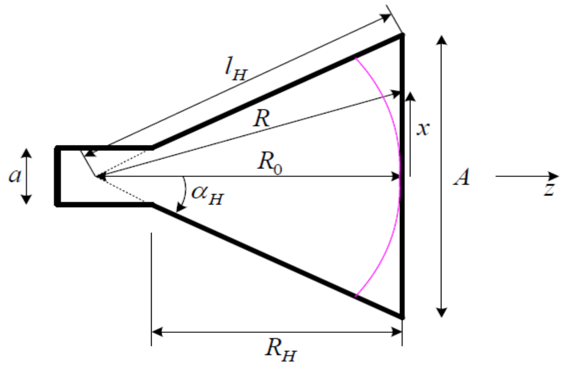

Figure 1: Geometry of H-plane sectoral horn

Where, l_H = Slant length of the horn, R_0 = Straight length of the horn, A = Aperture, α_H = Flare angle, R_H = Flare length and a = Waveguide height

2.2 Field Equations: The derivations of E and H field equations of H-plane sectoral horn are given in [6]. These equations are extracted and shown at Equ. (1) and Equ. (2) for ready reference.

$$F_E(\theta) = \left(\frac{1+\cos\theta}{2}\right)\left[\frac{\sin\left(0.5\beta b.\sin\theta.\sin\phi\right)}{0.5\beta b.\sin\theta.\sin\phi}\right] \quad (1)$$

$$F_H(\theta) = \left(\frac{1+\cos\theta}{2}\right).f_H(\theta) \quad (2)$$

Where

$$f_H(\theta) \propto \int_{-A/2}^{+A/2} \cos\left(\frac{\pi x'}{A}\right) e^{-j\beta\sqrt{R_0^2 + x'^2}} e^{j\beta x' \sin\theta} dx'$$

2.3 Directivity: The directivity of H-plane sectoral horn antennas is calculated using following procedure [6 -7, 9].

Step-1: Calculation of X using the formula

$$X = \frac{A}{\lambda}\sqrt{\frac{50}{l_H/\lambda}} \quad (3)$$

Step-2: Using the value of X , we have calculated G_H from "Fig. 2", since X > 2. For X < 2, we need to calculate G_H using Equ. (4).

$$G_H = \frac{32}{\pi} X \quad (4)$$

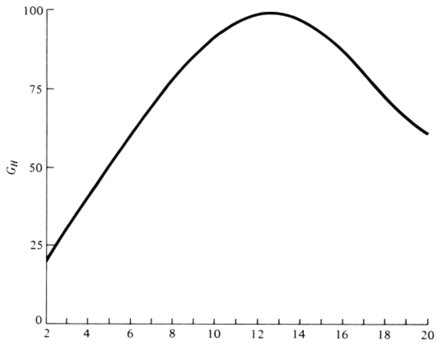

Figure 2: G_H as a function of X

Step-3: Now we have calculated D_H and gain using the following equations

$$D_H = \frac{b}{\lambda} \frac{G_H}{\sqrt{\frac{50}{l_H/\lambda}}} \quad (5a)$$

Gain in dB = $10\log(D_H)$ (5b)

2.4 Array Gain: The array gain with N elements is given [5, 14] by

$$G_{Array} = G_{element} + 10\log(N) \quad (6)$$

2.5 V.S.W.R: The V.S.W.R of the waveguide fed horn element is given [7] by

$$Z(z_i) = Z_0 e^{(\alpha z_i)}, z_i = \frac{iR_H}{n}, \alpha = \frac{1}{R_h}\ln\left(\frac{R_H}{Z_0}\right) \quad (7)$$

Where ' z_i ' the impedance of each section of the horn and 'n' is the total number of sections of the horn.

3. Design Calculations & Simulations:

3.1 Specifications of Array: The specifications of linear array of H-plane sectoral horns with 8 elements are tabulated at Table-1.

Table 1: Design Specifications of Array

S.No	Parameter	Linear array of H-plane sectoral horns
1.	Frequency range	2-6 GHz
2.	No of elements	8
3.	V.S.W.R Max.	3:1
4.	Gain (Min.)	14.3 dBi
5.	3-dB beam width (Az & El)	5-20°
6.	Power handling of element	100 Watts CW
7.	Impedance	50 Ω
8.	Connectors	N type or SMA

3.2 Design Calculations of the Element: Based on the above requirements, the design parameters of H-plane sectoral horn element at 2 GHz are calculated and given at Table-2 [12].

Table 2: Design Calculations of the Element

D_H (dBi)	D_H	G_H	X	A	R_0	l_H
5.7	3.7	95	13.4 mm	494.9mm	450 mm	450 mm

3.3 Simulation of Array: The arrangement of the array of H-plane sectoral horns is shown at "Fig. 3".

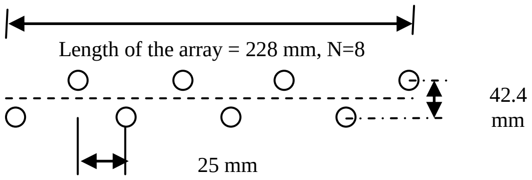

Figure 3: Arrangement of elements of linear array of H-plane sectoral horns

The elements of the array are arranged symmetrically on both sides of the center line without loss of generality to meet the spacing requirement of the elements of the array (i.e. 25 mm which is < λ/2 @ 6 GHz) to avoid grating lobes. The simulations have been carried out in the following ways.

- ✓ with Linear array of eight sectoral horns (Model-1)
- ✓ with Linear array of eight sectoral horns with hybrid tapering and dual wire loadingon aperture (Model-2)
- ✓ with Linear array of eight sectoral horns with hybrid tapering, dual wire laoding and insertion of parabolic lens(Model-3)
- ✓ with Linear array of eight sectoral horns with hybrid tapering, dual wire laoding andinsertion of dielectric slabs (Model-4)

The above models are simulated in solid works software and shown below at "Fig. 4" to "Fig. 7".

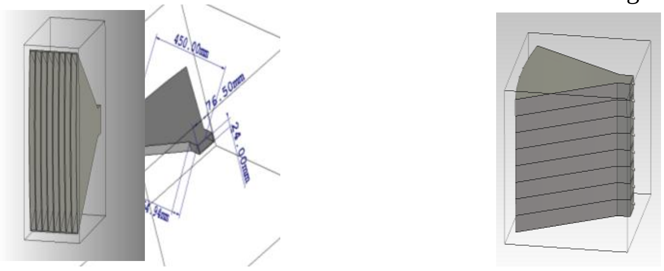

Figure 4: Solid-Model of 2-6GHz H-plane 8-element array with linear tapering (Model-1)

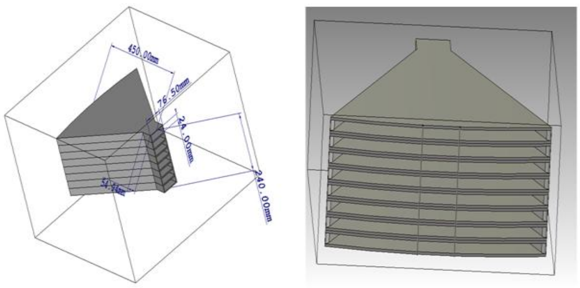

Figure 5: Solid-Model of 2-6GHz H-plane 8-element array with hybrid tapering and dual wire loading (Model-2)

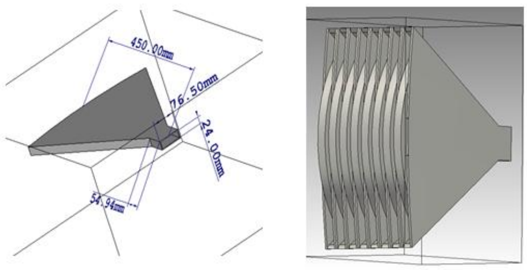

Figure 6: Simulated Model with hybrid tapering, dual wire loading on aperture and insertion of parabolic dielectric lens of linear array of H-plane sectoral horns (Model-3)

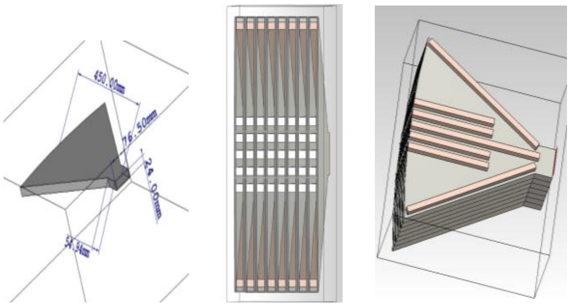

Figure 7: Simulated Model with hybrid tapering, dual wire loading on aperture and insertion of dielectric slabs of linear array of H-plane sectoral horns

In “Figure 4”, the aperture of horn is flared as per standard design procedures.

In “Figure 5”, the linear array of horns is simulated with hybrid tapering [9, 11] and dual wire loading on the aperture. A pair of brass wires of 1.4 mm diameter with λ/2 apart at the center on the aperture have created a large wave front and exhibited improvement in matching impedance of the waveguide impedance (Z_g) at low frequencies. The separation between these wires on the aperture is optimized in the simulation. The improvement in V.S.W.R is observed in the simulation with this configuration.

In “Figure 6”, the linear array of horns with hybrid tapering, dual wire loading and insertion of parabolic dielectric lens in the aperture is simulated. The improvement in gain is observed in the simulation in this configuration.

In “Figure 7”, the linear array of horns with hybrid tapering, dual wire loading and insertion of dielectric slabs in the horn body is simulated. The insertion of dielectric slabs has improved the side lobe levels in the radiation patterns.

3.4 Simulated results of V.S.W.R: The simulated V.S.W.R of 5th element of the array for the above four cases are plotted below at “Fig. 8” to “Fig. 11” respectively.

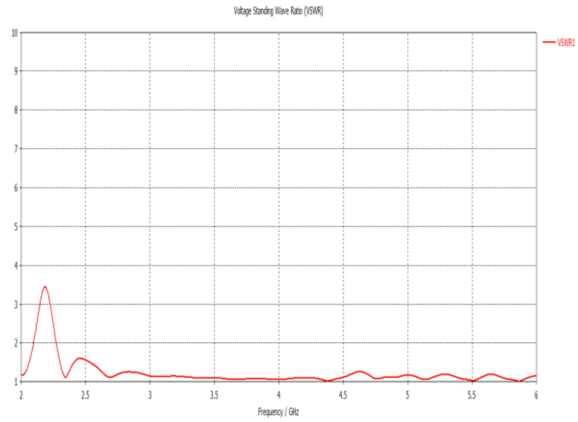

Figure 8: Simulated V.S.W.R of 2-6GHz H-plane 8-element array with linear tapering (Model-1)

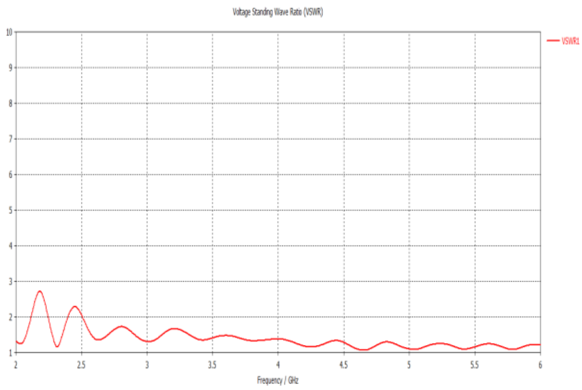

Figure 9: Simulated V.S.W.R of 2-6GHz H-plane 8-element array with hybrid tapering and dual wire loading (Model-2)

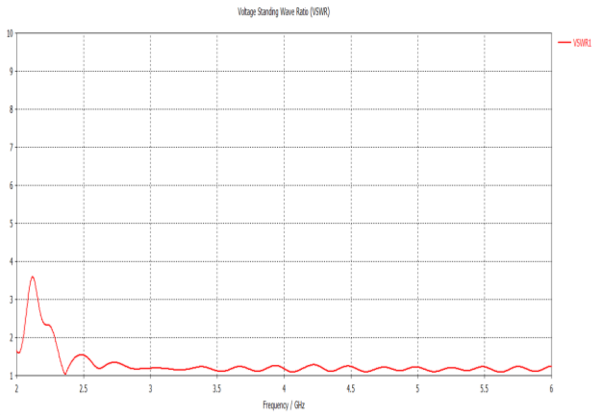

Figure 10: Simulated V.S.W.R of hybrid tapering, dual wire loading on aperture and insertion of parabolic dielectric lens of linear array of H-plane sectoral horns (Model-3)

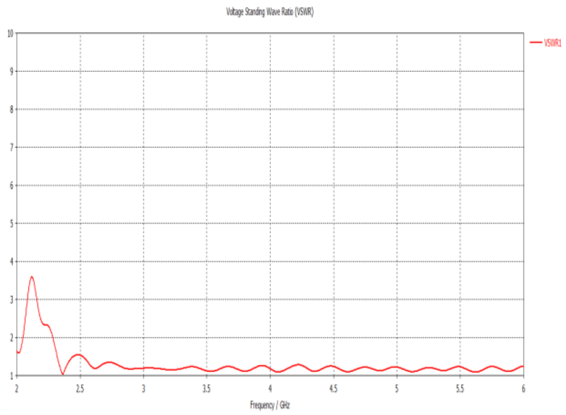

Figure 11: Simulated V.S.W.R of hybrid tapering, dual wire loading on aperture and insertion of dielectric slabs in the linear array of H-plane sectoral horns (Model-4)

3.5 Simulated Results of Radiation Diagrams: The radiation pattern is simulated for the center port of the array, with phase difference between all the ports of the elements is equal, so that maximum radiation is occurred at bore-sight. However, if the phase difference is varied by connecting Rotman lens, then the beam scans between the scan angles of ±45 degrees. The simulated radiation patterns of Model-1 array are shown from "Fig. 12" to "Fig. 20".

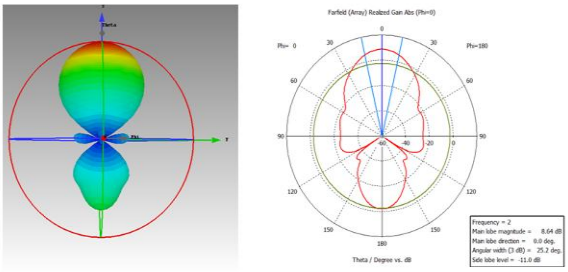

Figure 12: Simulated radiation pattern (Az) at 2 GHz

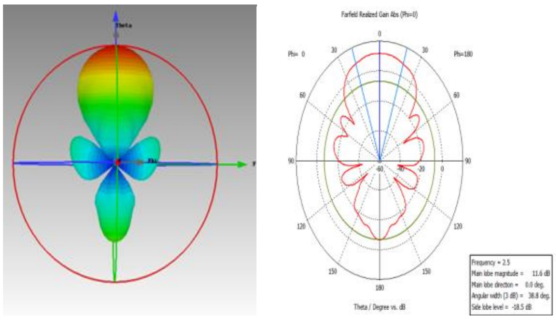

Figure 13: Simulated Radiation Pattern (Az) at 2.5GHz

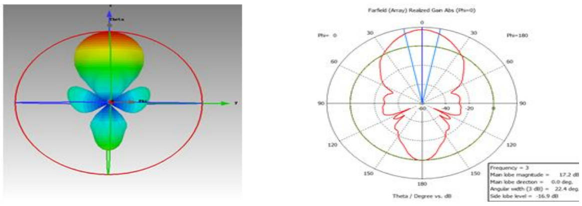

Figure 14: Simulated Radiation Pattern (Az) at 3GHz

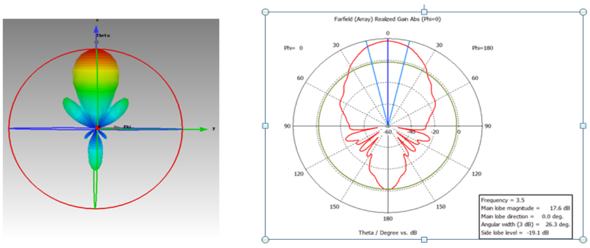

Figure 15: Simulated Radiation Pattern (Az) at 3.5GHz

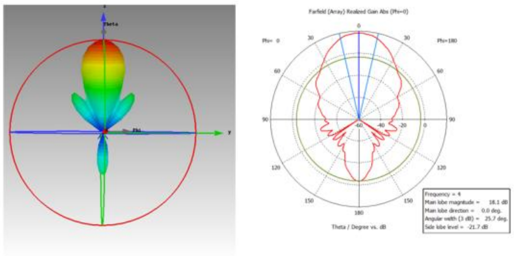

Figure 16: Simulated Radiation Pattern (Az) at 4GHz

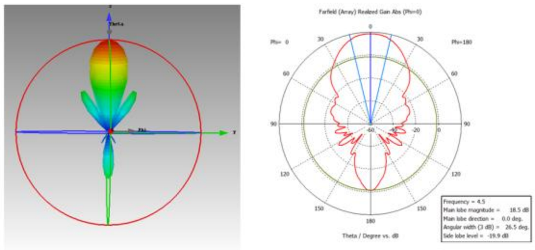

Figure 17: Simulated Radiation Pattern (Az) at 4.5GHz

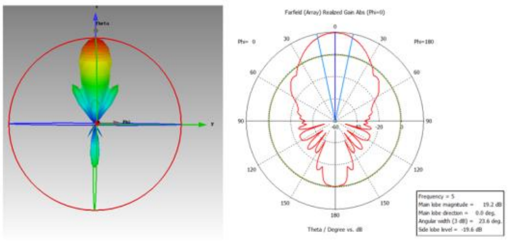

Figure 18: Simulated Radiation Pattern (Az) at 5GHz

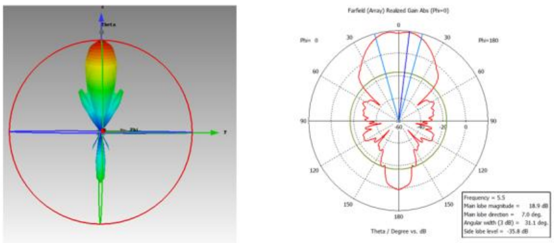

Figure 19: Simulated Radiation Pattern (Az) at 5.5 GHz

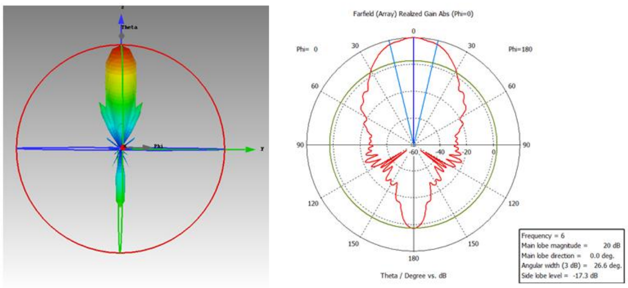

Figure 20: Simulated Radiation Pattern (Az) at 6 GHz

The simulated radiation patterns of Model-2 are shown from "Fig. 21" to "Fig. 29".

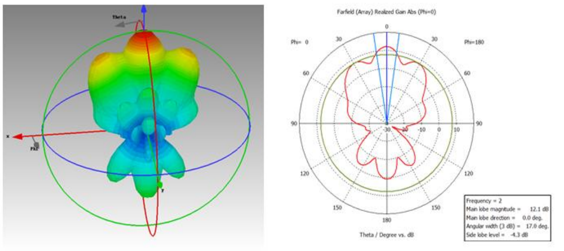

Figure 21: Simulated radiation pattern (Az) at 2 GHz

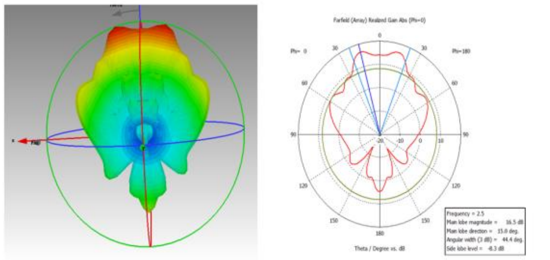

Figure 22: Simulated Radiation Pattern (Az) at 2.5GHz

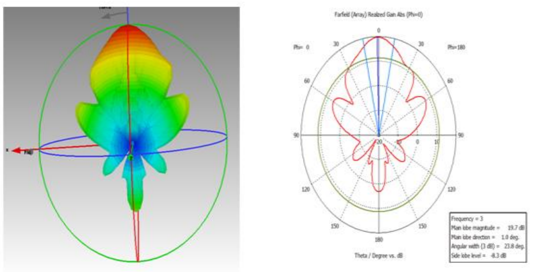

Figure 23: Simulated Radiation Pattern (Az) at 3GHz

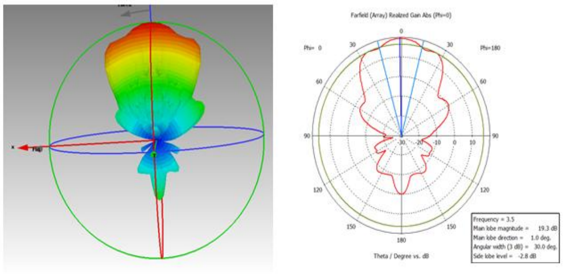

Figure 24: Simulated Radiation Pattern (Az) at 3.5GHz

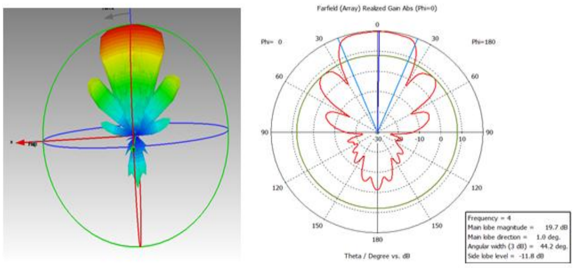

Figure 25: Simulated Radiation Pattern (Az) at 4GHz

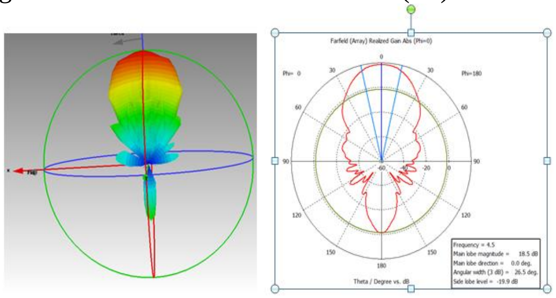

Figure 26: Simulated Radiation Pattern (Az) at 4.5GHz

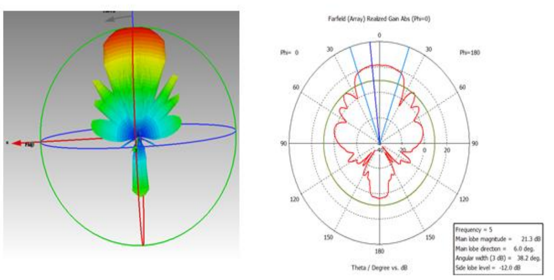

Figure 27: Simulated Radiation Pattern (Az) at 5GHz

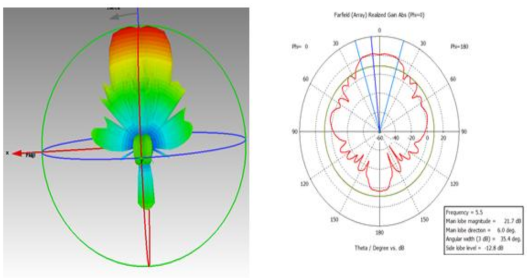

Figure 28: Simulated Radiation Pattern (Az) at 5.5 GHz

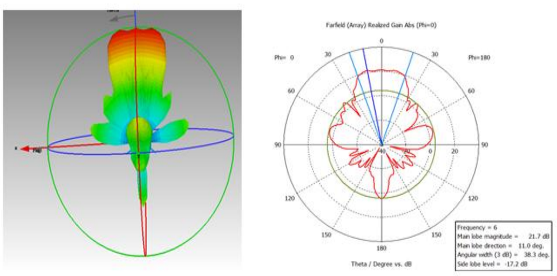

Figure 29: Simulated Radiation Pattern (Az) at 6 GHz

The simulated radiation patterns of Model-3 are shown from “Fig. 30” to “Fig. 38”.

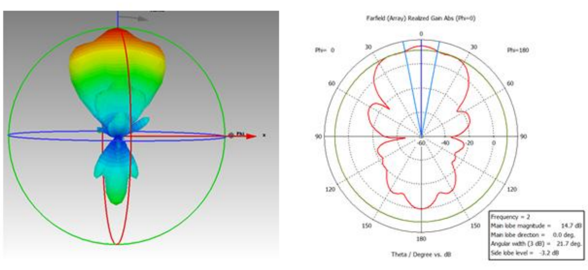

Figure 30: Simulated radiation pattern (Az) at 2 GHz

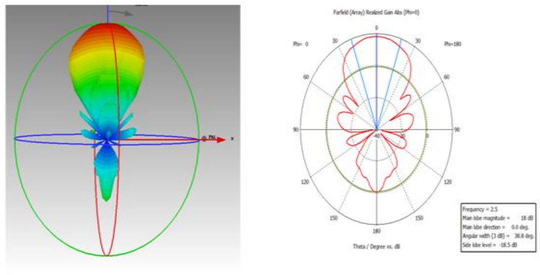

Figure 31: Simulated Radiation Pattern (Az) at 2.5GHz

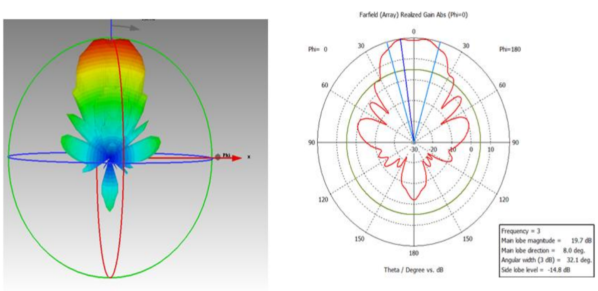

Figure 32: Simulated Radiation Pattern (Az) at 3GHz

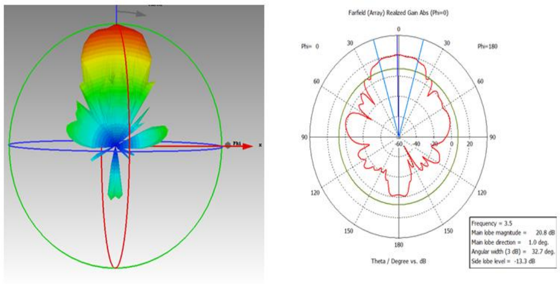

Figure 33: Simulated Radiation Pattern (Az) at 3.5GHz

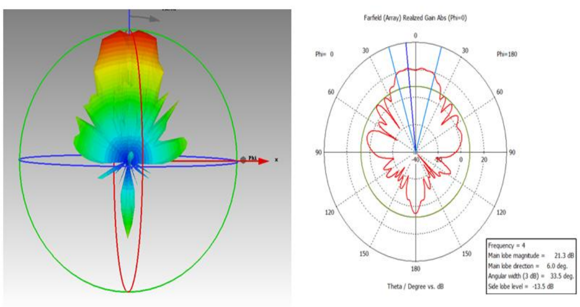

Figure 34: Simulated Radiation Pattern (Az) at 4GHz

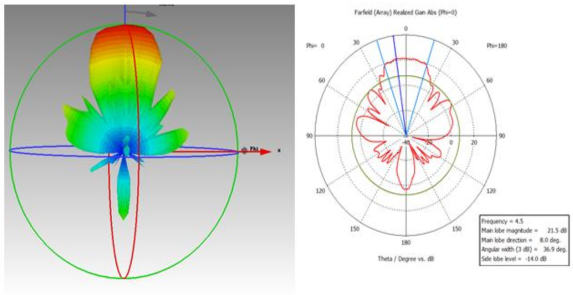

Figure 35: Simulated Radiation Pattern (Az) at 4.5GHz

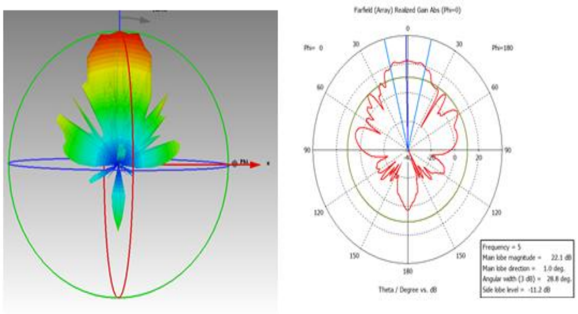

Fig. 36: Simulated Radiation Pattern (Az) at 5GHz

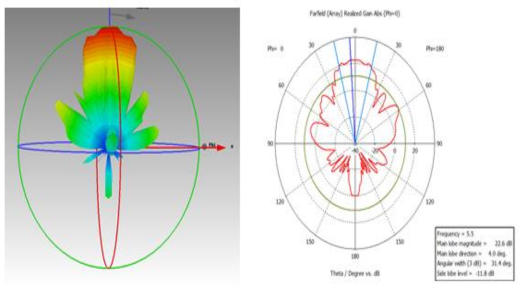

Fig. 37: Simulated Radiation Pattern (Az) at 5.5 GHz

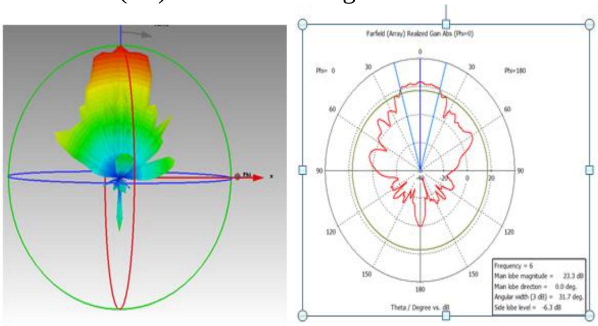

Figure 38: Simulated Radiation Pattern (Az) at 6 GHz

The simulated radiation patterns of Model-4 are shown at "Fig. 39" to "Fig. 47".

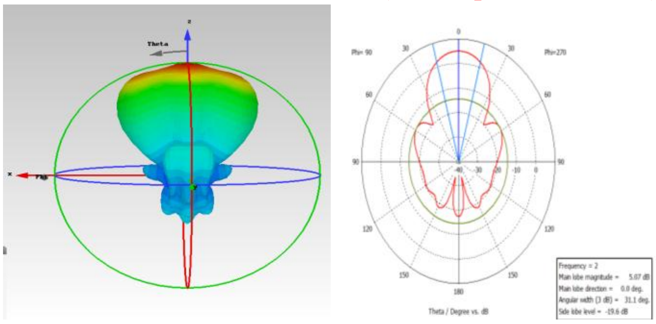

Figure 39: Simulated Radiation Pattern (Az) at 2 GHz

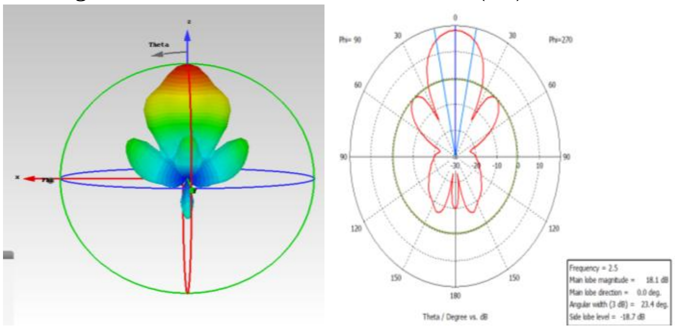

Figure 40: Simulated Radiation Pattern (Az) at 2.5 GHz

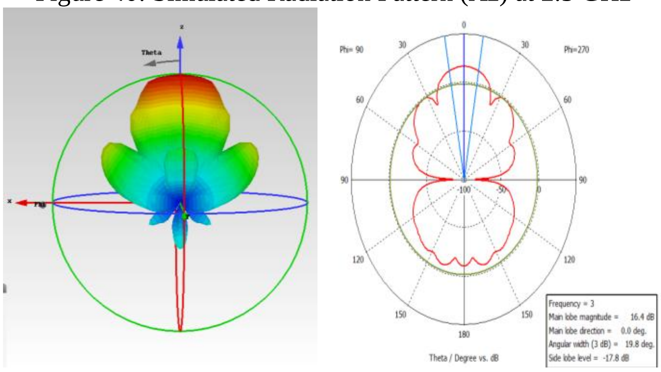

Figure 41: Simulated Radiation Pattern (Az) at 3.0 GHz

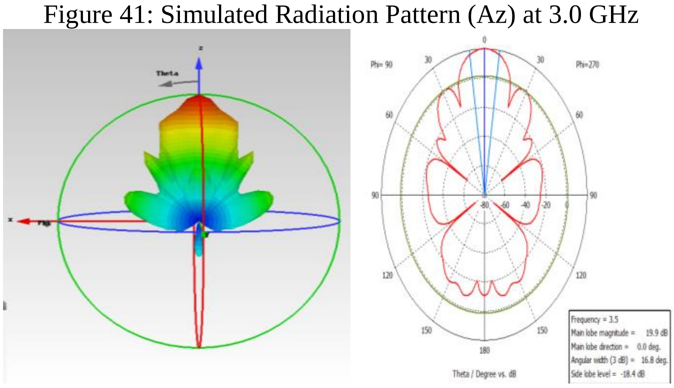

Figure 42: Simulated Radiation Pattern (Az) at 3.5 GHz

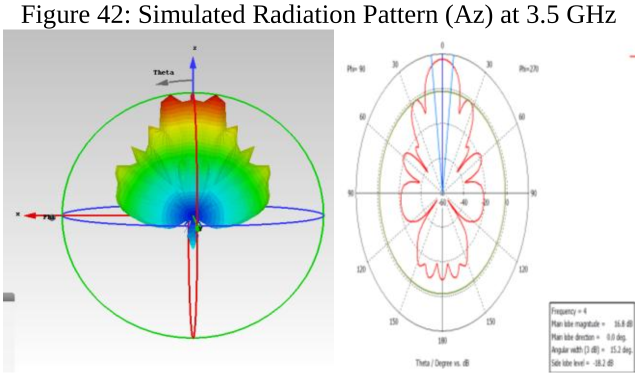

Figure 43: Simulated Radiation Pattern (Az) at 4.0 GHz

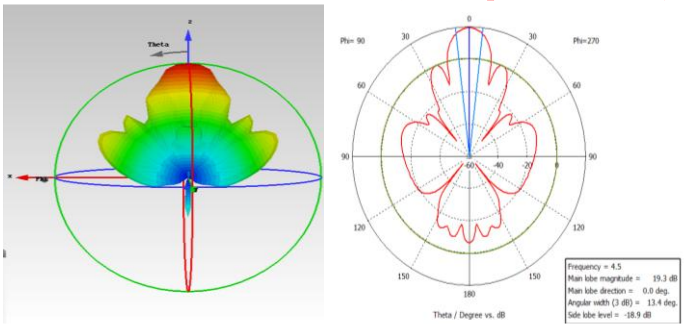

Figure 44: Simulated Radiation Pattern (Az) at 4.5 GHz

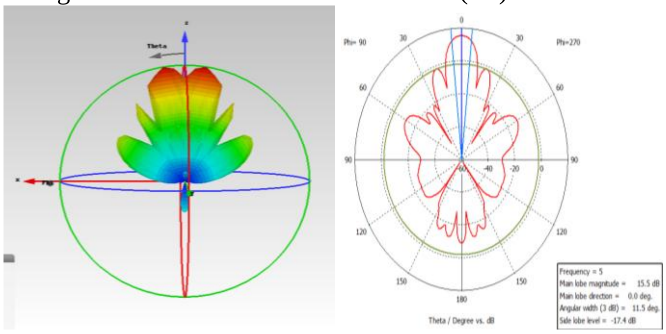

Figure 45: Simulated Radiation Pattern (Az) at 5.0 GHz

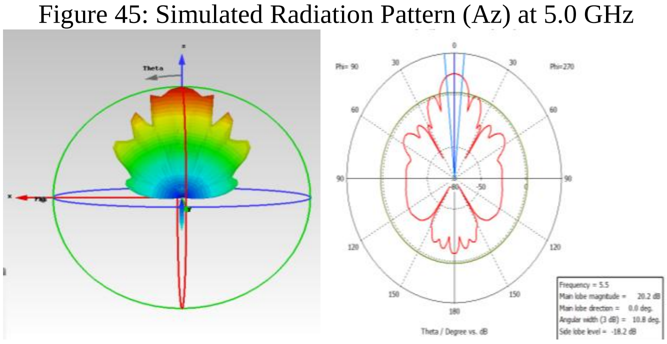

Figure 46: Simulated Radiation Pattern (Az) at 5.5 GHz

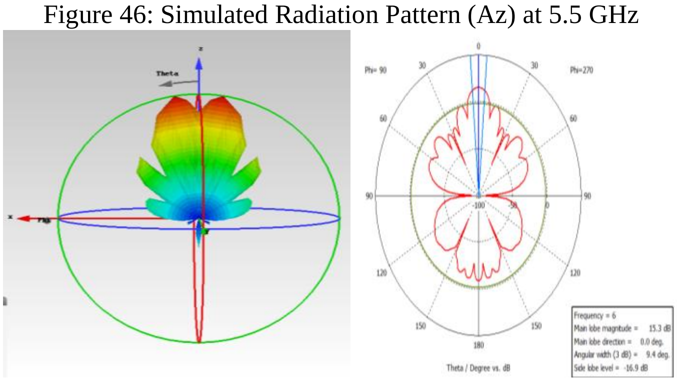

Figure 47: Simulated Radiation Pattern (Az) at 6.0 GHz

3.6 Simulated Results of Gain: The simulated gain plot for Model-1is shown in" Fig. 48".

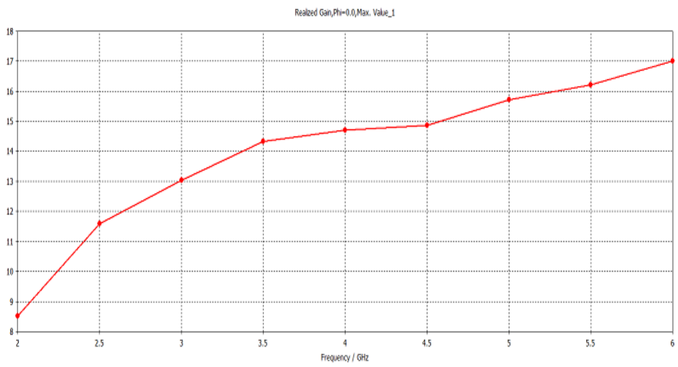

Figure 48: Simulated gain for Model-1

The simulated gain plot for Model-2 is shown in “Fig. 49”

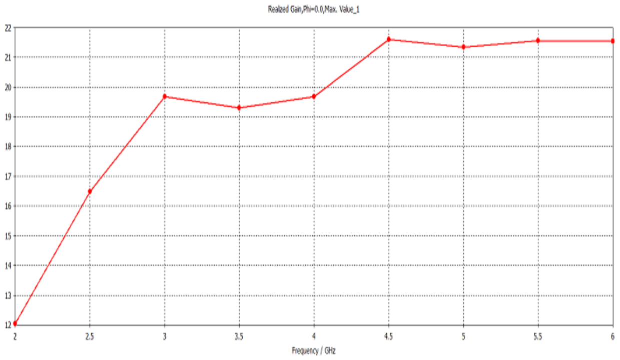

Figure 49: Simulated gain for Model-2

The simulated gain plot for Model-3 is shown in “Fig. 50”

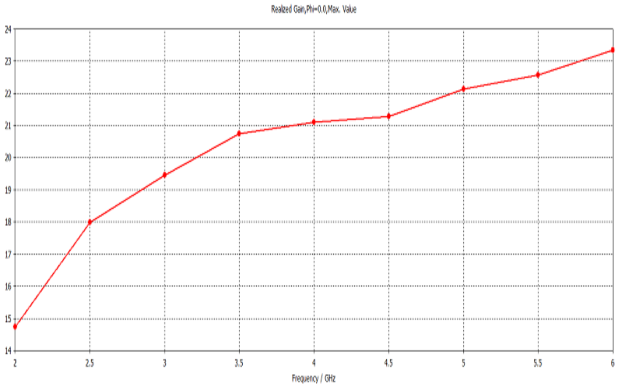

Figure 50: Simulated gain for Model-3

The simulated gain plot for Model-4 is shown in “Fig. 51”

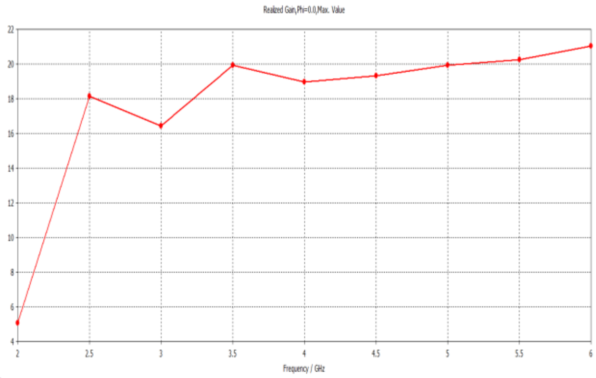

Figure 50: Simulated gain for Model-4

3.7 Summary of Simulation Results: The summary of the simulation results of four models are given below from Table-3 to 5.

Table 3: Summary of V.S.W.R of Model 1 to 4

S.No	**Type**	**V.S.W.R Max**
1.	Model-1	80% of the band <1.6:1 and Max 3.5:1
2.	Model-2	80% of the band <1.8:1 and Max 2.8:1
3.	Model-3	80% of the band <1.4:1 and Max 3.5:1
4.	Model-4	80% of the band <1.4:1 and Max 3.5:1

Table 4: Summary of Gain of Model 1 to 4

S.No	**Freq. in GHz**	**Gain in dBi**			
		Model-1	Model-2	Model-3	Model-4
1.	2.0	8.64	12.1	14.7	5.0
2.	2.5	11.5	16.5	18.0	18.0
3.	3.0	17.2	19.7	19.7	16.5
4.	3.5	17.6	19.3	20.8	20.0
5.	4.0	18.1	19.7	21.3	19.0

6.	4.5	18.5	18.5	21.5	19.5
7.	5.0	19.2	21.3	22.1	20.0
8.	5.5	18.9	21.7	22.6	20.2
9.	6.0	20.0	21.7	23.3	21.0

Table 5: Summary of S.L.L of Model 1 to 4

S.No	**Freq. in GHz**	**S.L.L in dB**			
		Model-1	Model-2	Model-3	Model-4
1.	2.0	-11.0	-4.3	-3.2	-19.6
2.	2.5	-18.5	-8.3	-18.5	-18.7
3.	3.0	-16.9	-8.3	-14.8	-17.8
4.	3.5	-19.1	-2.8	-13.3	-18.4
5.	4.0	-21.7	-11.8	-13.5	-18.2
6.	4.5	-19.9	-19.9	-14.0	-18.9
7.	5.0	-19.6	-12.0	-11.2	-17.4
8.	5.5	-35.8	-12.8	-11.8	-18.2
9.	6.0	-17.3	-17.2	-6.3	-16.9

4. Conclusion:

A 2-6 GHz linear array of eight sectoral horn elements using linear tapering, hybrid taper, dual wire loading, insertion of parabolic dielectric lens and insertion of dielectric slabs is simulated and compared for their performance and the results have been presented, which are useful for selection of the configuration for a particular applications.

5. Acknowledgement:

The authors are thankful to the engineers working at B.E.L for sparing their valuable time during the simulation. Each simulation has taken more than 12 hours and B.E.L has provided all the simulation facilities to carry out this work. Hence we extend our sincere thanks to management of B.E.L for providing all these facilities during the simulation work. We sincerely extend our gratitude to Prof. P Rajesh Kumar, HOD, ECE department, Andhra University, Hyderabad for his support during the preparation of the paper.

6. References:

1. Hans Schantz, "Antenna as Transducers and Antennas as transformer", in the title of Art and Science of Ultra Wide Band antennas" 1st edition, 2005, Artech publications
2. Pues H.F, "An impedance-matching techniques for increasing the bandwidth of micro strip antennas", Antennas and Propagation, IEEE transactions Vol. 37, issue 11, pages 1345-1354, ISSN: 0018-926X, 06 Aug 2002.
3. Constantine A Balanis, "Antenna Theory Analysis and design with multimedia CD", 3rd edition, Wiley India, reprint 2012.
4. Ronaldo O. dos Santos and Carlos Leonidas da S. S. Sobrinho, "FDTD method: Analysis of an one-dimensional array of H-plane sectoral horn antennas with dielectric lens", Revista Científica Periódica, Telecomunicações, Telecomunicações, Vol. 06, No.1, pp. 28-32, June 2003
5. Tae-Young Kim, Young-Min Yoon, Gun-Su Kim, and Boo-Gyoun Kim, "A Linear Phased Array Antenna Composed of Inductive Loaded Patch Antennas", IEEE Antennas and Wireless Propagation Letters (Volume: 10), 2011
6. Pues H.F, "An impedance-matching techniques for increasing the bandwidth of micro strip antennas", Antennas and Propagation, IEEE transactions Vol. 37, issue 11, pages 1345-1354, ISSN: 0018-926X, 06 Aug 2002.
7. P. M. Russo, R. C. Ruddock, and L. Peters, Jr., "A Method for Computing E-Plane Patterns of Horn Antennas," IEEE Trans. Antennas Propagat., Vol. AP-13, No. 2, pp. 219–224, March 1965.
8. J. S. Yu, R. C. Ruddock, and L. Peters, Jr., "Comprehensive Analysis for E-Plane of Horn Antennas by Edge Diffraction Theory," IEEE Trans. Antennas Propagat., Vol. AP-14, No.2, pp. 138–149, March 1966.
9. Ch Viswanadham, Prof P Mallikarjuna Rao, "Hybrid tapering and aperture smoothening for improving V.S.W.R of U.W.B Phased Array Horn Antenna for ECM applications", Feb 2016, presented at ICACCS, Coimbatore, India,
10. M. J. May bell and P. S. Simon, "Pyramidal Horn Gain Calculation with Improved Accuracy," IEEE Trans. Antennas Propagat., Vol. 41, No. 7, pp. 884–889, July 1993.
11. W. D. Burnside and C. W. Chuang, "An Aperture-Matched Horn Design," IEEE Trans. Antennas Propagat., Vol. AP-30, No. 4, pp. 790–796, July 1982.
12. Yun Zhao and Wen Wu, "Wideband and Low profile Linear array of H-plane horns on a conducting ground plane", Progress in Eletrcomagnetic Research Letters, Vol. 63, 71-77, 2016